© 2021. Published by The Company of Biologists Ltd | Journal of Cell Science (2021) 134, jcs256313. doi:10.1242/jcs.256313

RESEARCH ARTICLE

Substratum stiffness tunes membrane voltage in mammary epithelial cells

Brian B. Silver[1], Sherry X. Zhang[2], Emann M. Rabie[1,3] and Celeste M. Nelson[1,2,*]

ABSTRACT

Membrane voltage (V_m) plays a critical role in the regulation of several cellular behaviors, including proliferation, apoptosis and phenotypic plasticity. Many of these behaviors are affected by the stiffness of the underlying extracellular matrix, but the connections between V_m and the mechanical properties of the microenvironment are unclear. Here, we investigated the relationship between matrix stiffness and V_m by culturing mammary epithelial cells on synthetic substrata, the stiffnesses of which mimicked those of the normal mammary gland and breast tumors. Although proliferation is associated with depolarization, we surprisingly observed that cells are hyperpolarized when cultured on stiff substrata, a microenvironmental condition that enhances proliferation. Accordingly, we found that V_m becomes depolarized as stiffness decreases, in a manner dependent on intracellular Ca^{2+}. Furthermore, inhibiting Ca^{2+}-gated Cl^- currents attenuates the effects of substratum stiffness on V_m. Specifically, we uncovered a role for cystic fibrosis transmembrane conductance regulator (CFTR) in the regulation of V_m by substratum stiffness. Taken together, these results suggest a novel role for CFTR and membrane voltage in the response of mammary epithelial cells to their mechanical microenvironment.

KEY WORDS: Mechanical stress, Tissue morphodynamics, Bioelectricity

INTRODUCTION

Membrane voltage (V_m) is defined as the difference between the electric potential in the cytoplasm and that in the surrounding extracellular medium (Yang and Brackenbury, 2013). V_m is associated with several behaviors often dysregulated in cancer, including apoptosis, proliferation and phenotypic plasticity (Levin, 2014). In addition to regulating processes at the cellular level, gradients of V_m can form across populations of cells (bioelectricity) that profoundly impact growth at the tissue level during regeneration, organogenesis and tumorigenesis (Adams et al., 2007; Beane et al., 2011; Chernet and Levin, 2013; Sundelacruz et al., 2009; Yang and Brackenbury, 2013). It should, therefore, be possible to exploit bioelectric signals in order to reprogram ailments such as cancer or to induce the repair of damaged organs. Artificially manipulating V_m results in dramatic tissue-level changes, including ectopic organ formation and tumor suppression (Beane et al., 2011, 2013; Chernet and Levin, 2014; Pai et al., 2012). As a result, it will be useful to understand the biochemical machinery that transduces bioelectric signals into physiological states, as well as the extracellular stimuli that trigger a cell to change its V_m.

V_m generally ranges from 0 mV to −90 mV; proliferative and cancerous cells are thought to be more positively charged (depolarized) than quiescent or resting cells, which are thought to be more negatively charged (hyperpolarized) (Adams and Levin, 2013). However, V_m is not a static cellular property. Cells use ion channels, pumps, transporters and gap junctions to modulate V_m. These channels may be gated in response to ion concentration, V_m itself (voltage-gated ion channels) (Adams and Levin, 2006) or mechanical forces (Martinac, 2004; Silver et al., 2020). V_m is thus a dynamic property that is impacted by the surrounding cellular microenvironment. However, it is unclear what microenvironmental signals specify the V_m of cells within a tissue.

Although the mechanical microenvironment plays an instructive role at both the cellular and tissue levels (Chowdhury et al., 2010; Engler et al., 2006; Ko et al., 2016; Kostic et al., 2009; Lee et al., 2012; Lee and Nelson, 2013; Provenzano et al., 2009; Tilghman et al., 2010; Ulrich et al., 2009; Zhang et al., 2011), and mechanosensitive ion channels can regulate the influx of cations in response to mechanical stimuli including stretch or compression (Coste et al., 2010; Gudipaty et al., 2017; Wu et al., 2017), the connections between tissue mechanics and V_m are only beginning to emerge. Cells sense the stiffness of their substratum through cell-surface receptors linked to the actomyosin cytoskeleton, akin to how we sense the rigidity of a surface using our muscles (Kobayashi and Sokabe, 2010). This enhances cytoskeletal tension (Katsumi et al., 2004). Substratum stiffness has been found to regulate cellular behaviors including proliferation (Ulrich et al., 2009), apoptosis (Chiu et al., 2007; Wang et al., 2000; Zhang et al., 2011), differentiation (Engler et al., 2006) and epithelial–mesenchymal transition (EMT) (Lee et al., 2012). Substratum stiffness and cytoskeletal tension have also been found to regulate Ca^{2+} influx (Chiu et al., 2007; Kim et al., 2009; Pathak et al., 2014). This observation suggests a possible link between matrix rigidity and V_m, as some mechanosensitive ion channels that permit Ca^{2+} influx are nonspecific (Wu et al., 2017) and thus allow the influx of other positively charged ions including K^+ and Na^+. However, it remains unclear whether V_m is regulated by the mechanical properties of the microenvironment.

Here, we examined the relationship between substratum stiffness and V_m in mammary epithelial cells. We found that cells cultured on soft substrata with compliances reminiscent of the normal mammary gland were substantially more depolarized (more positively charged) than cells cultured on stiff substrata with compliances similar to mammary tumors. We observed substratum-induced regulation of V_m in several cell lines, including functionally normal and tumorigenic mouse and human mammary epithelial cells. This regulation appears to occur in a switch-like manner, wherein a

[1]Department of Molecular Biology, Princeton University, Princeton, NJ 08544, USA. [2]Department of Chemical & Biological Engineering, Princeton University, Princeton, NJ 08544, USA. [3]Graduate School of Biomedical Sciences, Rutgers Robert Wood Johnson Medical School, Piscataway, NJ 08854, USA.

*Author for correspondence (celesten@princeton.edu)

C.M.N., 0000-0001-9973-8870

Handling Editor: Andrew Ewald
Received 26 October 2020; Accepted 2 June 2021

Journal of Cell Science (2021) 134, jcs256313. doi:10.1242/jcs.256313

threshold level of stiffness is required to trigger hyperpolarization (a more negative charge). Subsequent increases in stiffness promoted further decreases in V_m. Finally, we uncovered a role for Ca^{2+}-gated Cl^- channels (CaCCs) in the mechanical regulation of V_m. A wide range of stimuli, including mechanical inputs, are believed to be involved in the gating of CaCCs (Slack-Davis et al., 2007). Cystic fibrosis transmembrane conductance regulator (CFTR) is an epithelial Cl^- channel primarily known for its dysfunction in cystic fibrosis (Sheppard and Welsh, 1999), but this channel is also expressed by mammary epithelial cells and has been implicated in breast cancer (Blaug et al., 2001). CFTR can be activated indirectly by increased intracellular Ca^{2+} in a pathway involving phosphorylation of the channel by protein kinase A, resulting in the flow of Cl^- out of the cell (depolarization) (Brennan et al., 2016). We observed that inhibiting either CFTR or Ca^{2+} release-activated channels (CRACs) abolished the ability of substratum stiffness to tune V_m. Taken together, these observations reveal that the mechanical microenvironment regulates the V_m of mammary epithelial cells through differential gating of CFTR in a Ca^{2+}-dependent manner.

RESULTS

To examine how V_m is affected by the mechanical compliance of the microenvironment, we used the fluorescent voltage-reporter dye bis-(1,3-dibutylbarbituric acid)-trimethine oxonol [$DiBac_4(3)$]. This anionic compound more easily enters the plasma membrane of less negatively charged (depolarized) cells, yielding stronger fluorescence. More negatively charged (hyperpolarized) cells show weaker fluorescence, with each 1% change in fluorescence intensity corresponding to 1 mV change in V_m (Bräuner et al., 1984; Klapperstück et al., 2013; Silver et al., 2020; Yamada et al., 2001). We cultured EpH4 cells, a phenotypically normal mouse mammary epithelial cell line, overnight on soft [elastic modulus (E) ∼130 Pa] or stiff (E ∼4020 Pa) polyacrylamide gels, which mimic the stiffnesses of normal and tumorigenic mammary tissue, respectively (Paszek et al., 2005). We found that cells cultured on stiff substrata exhibited weaker $DiBac_4(3)$ signal than those cultured on soft substrata (Fig. 1A,B), suggesting that they were hyperpolarized compared to cells on soft microenvironments.

Gramicidin is a peptide that inserts into the plasma membrane and allows ions to pass freely between the cytoplasm and the external medium (Kelkar and Chattopadhyay, 2007), thus setting cellular V_m to 0 mV. We used gramicidin as a control to calculate the V_m of cells on the different microenvironments. In cells cultured on stiff substrata, treatment with gramicidin led to an increase in $DiBac_4(3)$ fluorescence intensity, consistent with our conclusion that cells were hyperpolarized on stiff microenvironments (Fig. 1B). Curiously, the fluorescence of gramicidin-treated (V_m=0 mV) cells on stiff substrata was slightly lower than that of cells on soft substrata, perhaps due to differences in intracellular morphology on the different microenvironments. For this reason, we used a separate gramicidin-treated control for each substratum stiffness in order to calculate V_m. This analysis confirmed that cells cultured on stiff substrata are hyperpolarized (−53.9 mV) compared to those on soft substrata (−1.6 mV) (Fig. 1C).

To determine whether the response of V_m to stiffness is altered after oncogenic transformation, we examined the Ras-transformed EpH4 mammary epithelial cell line, EpRas (Oft et al., 1996). Similar to EpH4 cells, EpRas cells cultured on stiff substrata are hyperpolarized compared to cells cultured on soft substrata (Fig. 1C). SCp2 and SCg6 are isogenic mouse mammary epithelial cell lines; SCg6 cells are larger and form invasive tumors upon injection into nude mice, in contrast to their smaller, nontumorigenic SCp2 counterparts (Desprez et al., 1993). We found that, in SCp2 and SCg6 cells, V_m is regulated by substratum stiffness to a similar extent as in EpH4 cells. We observed a similar trend in highly metastatic, tumorigenic murine 4T1 cells as well as in MCF10A human mammary epithelial cells. Altogether, these results suggest that V_m is regulated by substratum stiffness in several mammary epithelial cell lines, including those that are phenotypically normal (EpH4, SCp2, MCF10A) as well as those that are tumorigenic (EpRas, 4T1, SCg6).

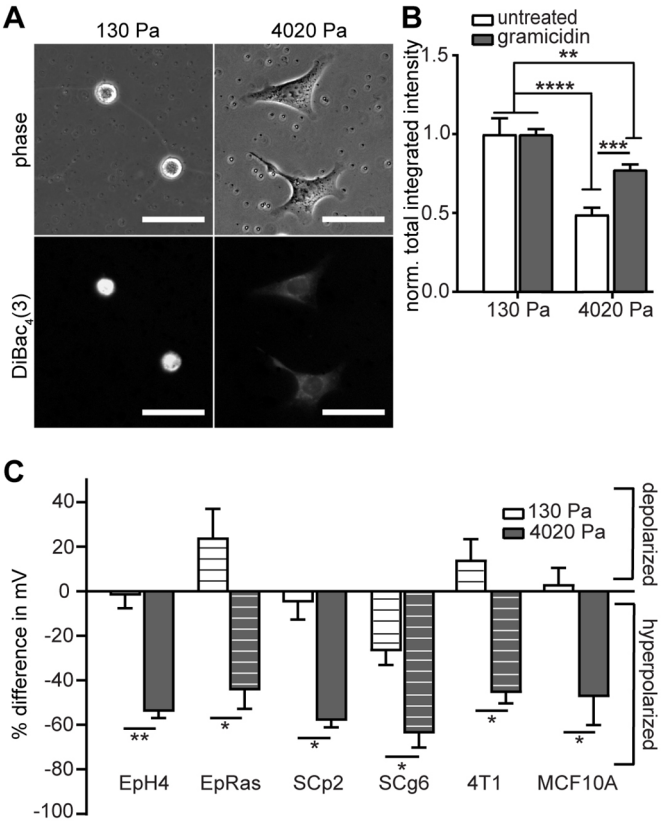

Fig. 1. Mammary epithelial cells cultured on stiff substrata are hyperpolarized compared to those on soft substrata. (A) EpH4 mouse mammary epithelial cells were cultured on soft (130 Pa) or stiff (4020 Pa) substrata and $DiBac_4(3)$ fluorescence was measured under each condition. (B) Background fluorescence was subtracted from the total integrated intensity measurements of images shown in A, and then normalized to the control. Fluorescence was compared quantitatively for cells on each substratum. (C) Membrane voltage (V_m) was calculated as the percentage difference between gramicidin-treated and untreated EpH4, EpRas, SCp2, SCg6, 4T1, and MCF10A cells cultured on each substratum; a 1% difference in fluorescence corresponds to a 1 mV change in V_m. Cancer cell lines are indicated by the striped bars. Scale bars: 50 µm. Shown are mean+s.d. *P<0.05; **P<0.01; ***P<0.001; ****P<0.0001; as determined by an unpaired parametric t-test with Welch's correction. N=3 independent replicates.

To define more precisely how V_m varies with substratum stiffness, we cultured EpH4 cells on polyacrylamide substrata of intermediate stiffnesses (E∼910 Pa and 2030 Pa) and measured V_m by comparing $DiBac_4(3)$ fluorescence to gramicidin-treated cells as described above. We found no significant difference in the V_m of cells cultured on 130 Pa and 910 Pa substrata (Fig. 2A). However, we observed a substantial and significant voltage drop (hyperpolarization) of −37 mV between 910 Pa and 2030 Pa. Between 2030 Pa and 4020 Pa, there was a lesser, but still significant, drop of an additional −17 mV. These data suggest that mammary epithelial cells become hyperpolarized above a threshold

Journal of Cell Science (2021) 134, jcs256313. doi:10.1242/jcs.256313

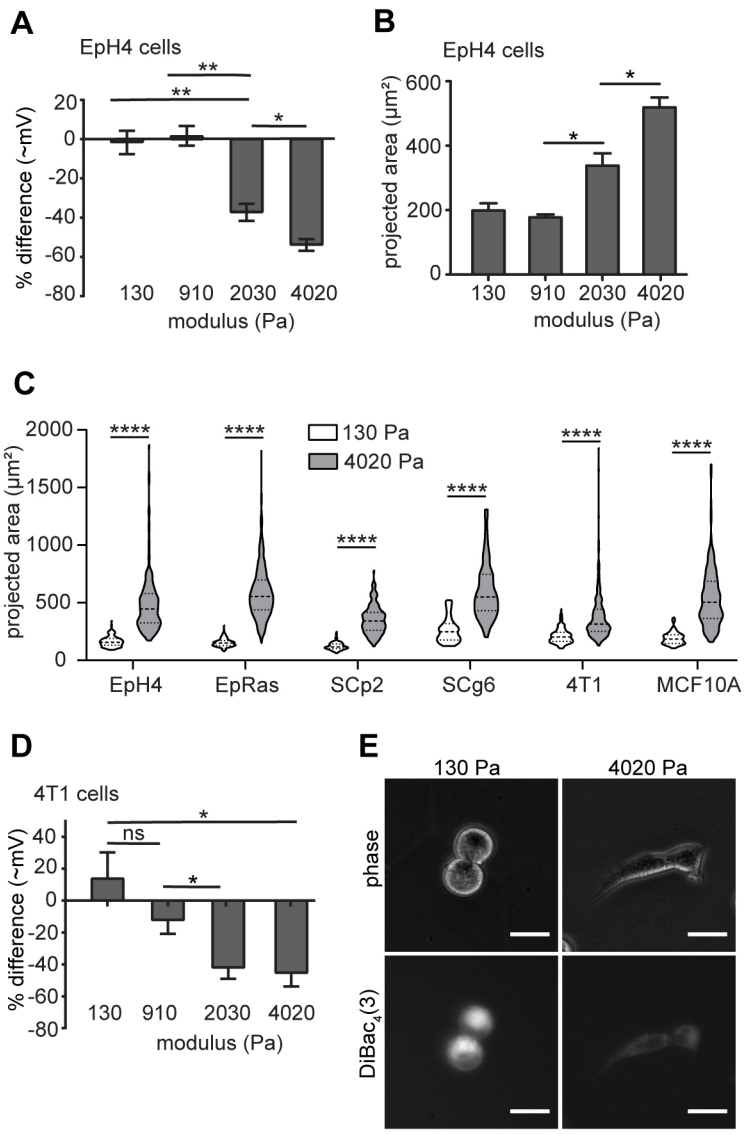

Fig. 2. A threshold substratum stiffness is required for mammary epithelial hyperpolarization. (A,B) V_m (A) and projected area (B) of EpH4 mouse mammary epithelial cells cultured on substrata of different stiffnesses. (C) Violin plots showing projected areas of different mammary epithelial cell lines on soft (130 Pa) or stiff (4020 Pa) substrata. Shown are distributions with indicated median and quartiles of the projected area of EpH4 (*n*=129, soft; *n*=184, stiff), EpRas (*n*=410 soft; *n*=561, stiff), SCp2 (*n*=74 soft; *n*=137, stiff), SCg6 (*n*=45, soft; *n*=54, stiff), 4T1 (*n*=245, soft; *n*=249, stiff) and MCF10A (*n*=90, soft; *n*=266, stiff) cells taken across three independent replicates each. (D) V_m of 4T1 cells cultured on substrata of different stiffnesses. (E) Phase-contrast and fluorescence images of 4T1 cells on soft or stiff substrata reveal increased $DiBac_4(3)$ fluorescence in cells cultured on soft substrata. Scale bars: 50 µm. Shown are mean+s.d. **P*<0.05; ***P*<0.01; *****P*<0.0001; ns, not significant; as determined by an unpaired parametric *t*-test with Welch's correction (A,B,D) or an unpaired Mann–Whitney test (C). *N*=3 independent replicates.

substratum stiffness. Curiously, the change in V_m correlated with a significant increase in projected cell area between 910 Pa and 2030 Pa (Fig. 2B). We observed that culture on stiff substrata correlated with a significant increase in projected cell area in all cell lines (Fig. 2C). We also observed a significant increase in hyperpolarization with increasing substratum stiffness in 4T1 cells (Fig. 2D,E).

To further investigate the relationship between cell spreading and V_m, we used microfabricated substrata (Tan et al., 2004) to control the projected area of mammary epithelial cells and measured the resulting V_m. This approach enabled us to compare round (~200 µm^2) with spread (~450 µm^2) cells (Fig. 3A–D), the projected areas of which were comparable to those of EpH4 cells cultured on soft or stiff microenvironments, respectively. We observed that round EpH4 (Fig. 3E,F) or 4T1 (Fig. 3G,H) cells were more depolarized than their spread counterparts. Differences in the degree of cell spreading could impact the height of a cell. However, cell height was only slightly decreased in EpH4 cells cultured on stiff substratum, and not in a manner proportional to projected cell area (Fig. S1). Furthermore, these modest differences in cell height did not affect the intensity of cells stained with a voltage-independent dye (Fig. S1). Together, these results suggest that substratum stiffness may regulate V_m, in part, by impacting the degree to which a cell spreads, which is controlled by cell-matrix adhesion and actomyosin contractility (Califano and Reinhart-King, 2010; Fu et al., 2010; Kong et al., 2005; Rhee et al., 2007).

Integrin-mediated activation of focal adhesion kinase (FAK; also known as PTK2) is a primary mechanism by which matrix compliance is transduced into changes in cell shape and phenotype (Guan, 2010; Provenzano et al., 2009). We used immunofluorescence analysis of phosphorylated, activated FAK (pFAK) to visualize and quantify focal adhesions in EpH4 and 4T1 cells cultured on soft or stiff substrata and round or spread microfabricated islands. EpH4 (Fig. 4A–E) and 4T1 (Fig. S2A–D) cells cultured on stiff substrata or fully spread on microfabricated islands formed more focal adhesions with larger total focal adhesion coverage per cell than those cultured on soft substrata or constrained to round islands. To determine whether signaling through FAK is required for stiffness-mediated regulation of V_m, we disrupted its activity using the small-molecule inhibitor PF-573228 (Ma et al., 2017a) (Fig. S2E) at a concentration that did not affect cell spreading (Fig. S2F). Treatment with PF-573228 increased the variability in V_m in cells cultured on soft and stiff substrata, without significantly affecting the mean V_m in either microenvironment

Journal of Cell Science (2021) 134, jcs256313. doi:10.1242/jcs.256313

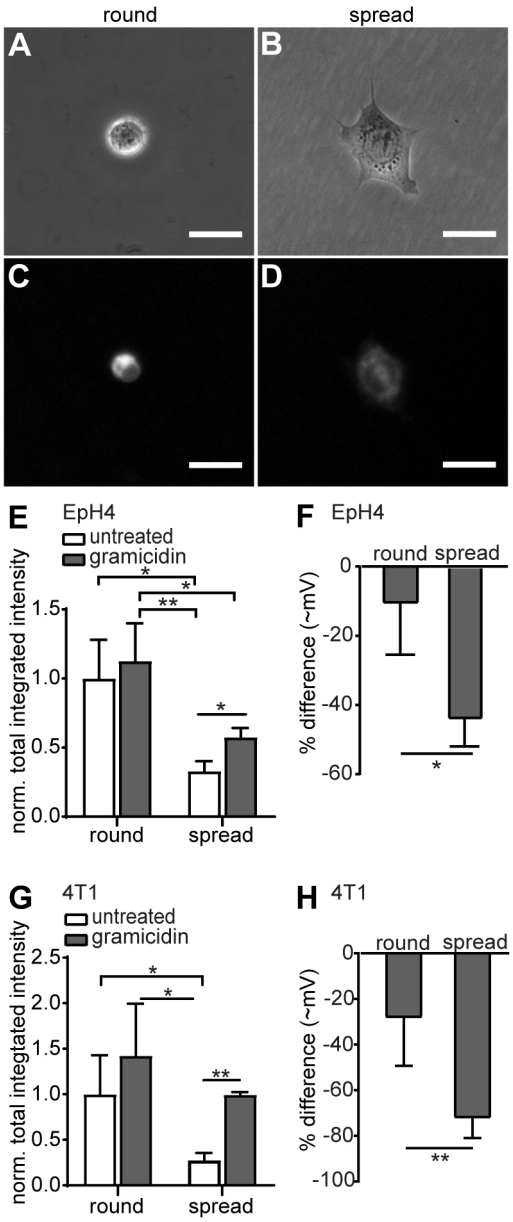

Fig. 3. V_m correlates with projected cell area. (A,B) Phase-contrast images of round (A) or spread (B) EpH4 cells cultured on micropatterned substrata. (C,D) $DiBac_4(3)$ fluorescence was measured for the round (C) and spread (D) EpH4 cells. (E–H) V_m was calculated for each condition by comparing the total integrated intensity of $DiBac_4(3)$ fluorescence in gramicidin-treated and untreated EpH4 (E,F) or 4T1 (G,H) cells, and normalizing to the untreated condition. Scale bars: 50 µm. Shown are mean+s.d. *P<0.05; **P<0.01; as determined by an unpaired parametric t-test with Welch's correction. N=3 independent replicates.

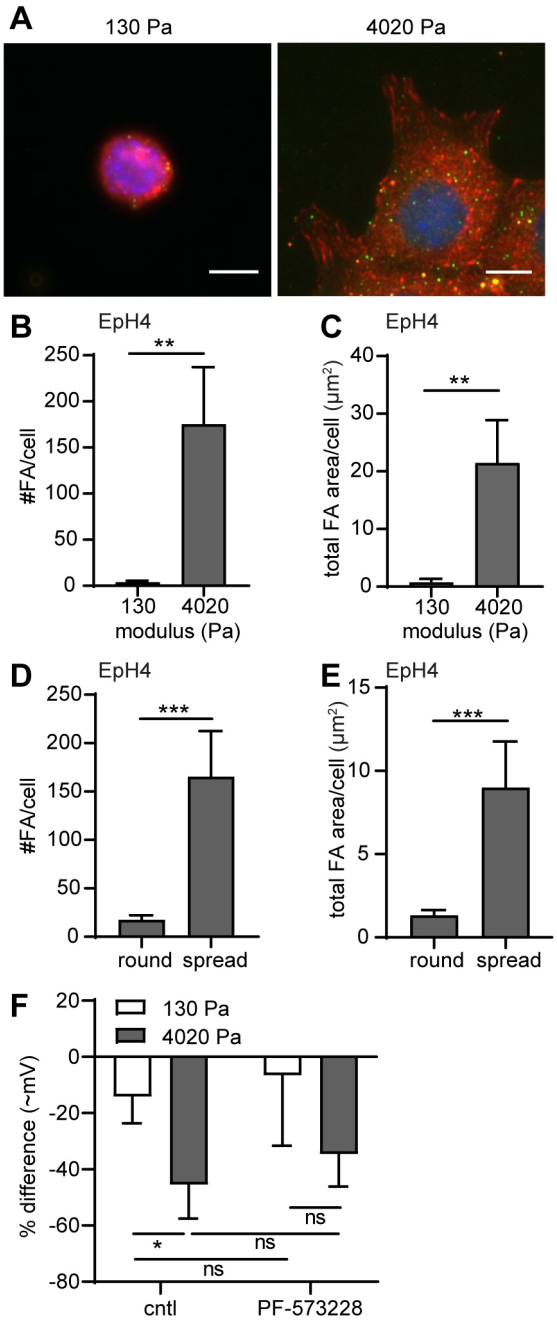

Fig. 4. The regulation of V_m by substratum stiffness is regulated, in part, by signaling through FAK. (A) Immunofluorescence analysis of focal adhesions in EpH4 cells cultured on soft or stiff substrata (blue, nuclei; red, vinculin; green, pFAK). Scale bars: 10 µm. (B,C) Mean number (B) and total area (C) of focal adhesions in EpH4 cells cultured on soft (n=54 cells) or stiff substrata (n=75 cells). (D,E) Mean number (D) and total area (E) of focal adhesions in round (n=15 cells) or spread (n=53 cells) EpH4 cells cultured on micropatterned substrata. (F) Inhibiting FAK significantly reduced the difference in V_m between EpH4 cells cultured on soft (n=110, control; n=84, PF-573228) versus stiff (n=595, control; n=429, PF-573228) substrata. Shown are mean+s.d. *P<0.05; **P<0.01; ***P<0.001; ns, not significant; as determined by an unpaired parametric t-test with Welch's correction. N=3 independent replicates.

(Fig. 4F), suggesting that FAK is required for cells to sense the stiffness of their underlying substratum and tune V_m. These data suggest that substratum stiffness signals through cell spreading and FAK to regulate V_m.

We next investigated other molecular mechanisms that might link mechanosensing and V_m. Piezo ion channels open in response to mechanical stimuli, including substratum stiffness (Wu et al., 2017). To determine whether Piezo1 plays a role in stiffness-induced changes in V_m, we treated EpH4 cells with the mechanosensitive ion-channel blocker $GdCl_3$ (Coste et al., 2010; Ermakov et al., 2010). Surprisingly, this treatment did not significantly impact V_m in cells cultured on soft or stiff substrata (Fig. S3A,B). We therefore investigated other types of channels. Large-pore channels such as pannexin1 and connexin hemichannels can be gated by mechanical force (Batra et al., 2012). The activity of

Journal of Cell Science (2021) 134, jcs256313. doi:10.1242/jcs.256313

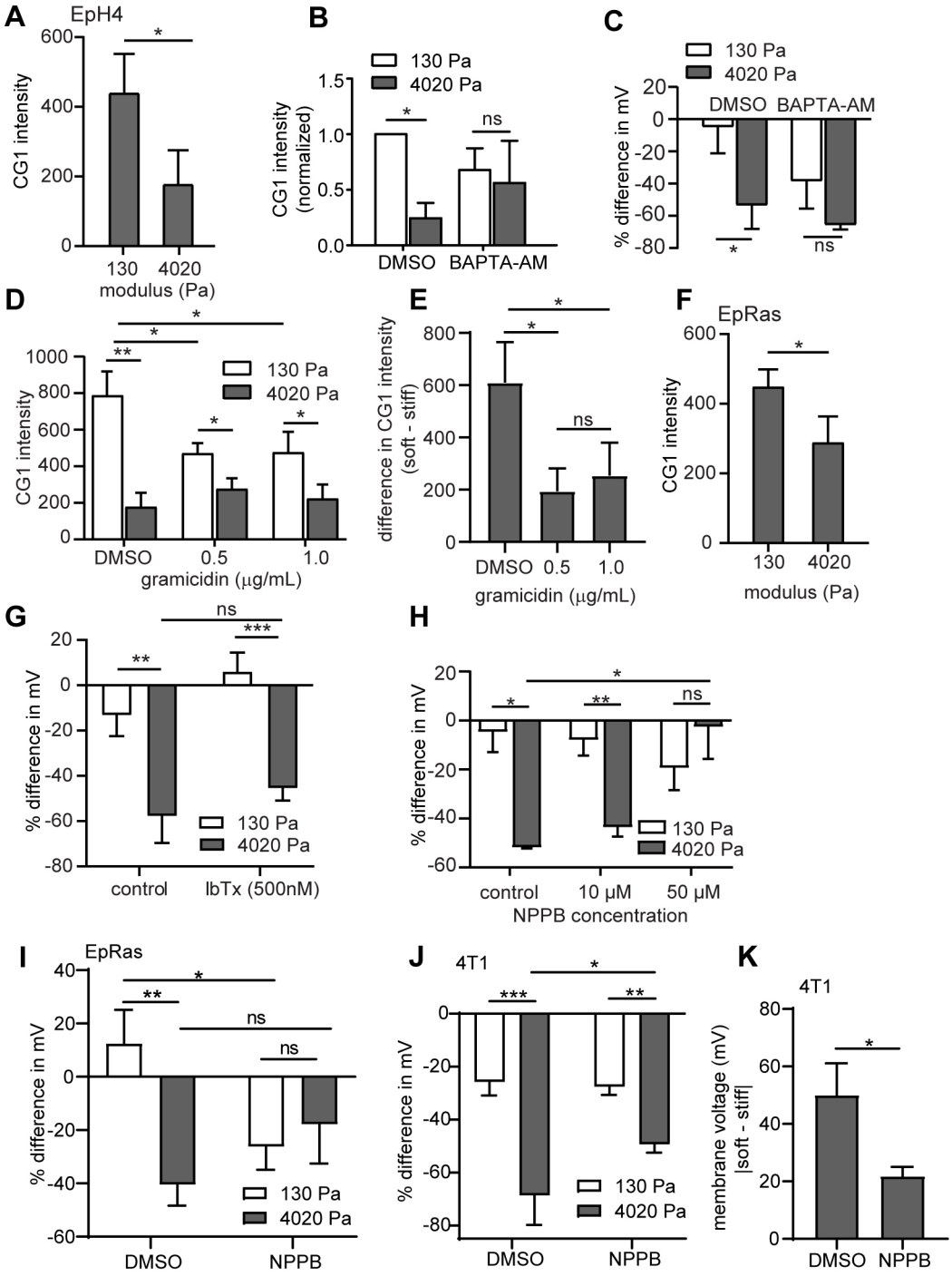

Fig. 5. Ca^{2+}-gated Cl^- currents are implicated in the regulation of V_m by substratum stiffness. (A) CG1 fluorescence in EpH4 cells cultured on soft or stiff substrata. (B) CG1 fluorescence of EpH4 cells cultured on soft or stiff substrata and treated with or without BAPTA-AM. Fluorescence values were normalized to control cells (DMSO) cultured on soft substrata. (C) V_m measurements of EpH4 cells cultured on soft or stiff substrata and treated with or without BAPTA-AM. (D) CG1 fluorescence in EpH4 cells cultured on soft or stiff substrata and treated with or without gramicidin. (E) Difference in CG1 fluorescence in EpH4 cells cultured on soft or stiff substrata and treated with or without gramicidin. (F) CG1 fluorescence in EpRas cells cultured on soft or stiff substrata. (G,H) V_m of EpH4 cells cultured on soft or stiff substrata in the presence or absence of iberiotoxin (IbTx) (G) or NPPB (H). (I,J) V_m of EpRas cells (I) or 4T1 cells (J) cultured on soft or stiff substrata in the presence or absence of NPPB. (K) Absolute difference in V_m between 4T1 cells cultured on soft or stiff substrata in the presence or absence of NPPB. Shown are mean+s.d. *P<0.05; **P<0.01; ***P<0.001; ns, not significant; as determined by an unpaired parametric t-test with Welch's correction (A,C-K) or by a one-sample unpaired t-test between control cells cultured on a soft substratum (hypothetical value of 1.0) and control cells cultured on a stiff substratum (B). N=3 independent replicates.

these channels can be visualized by uptake of the cationic vital dye YoPro in nonapoptotic cells (Patel et al., 2014). However, we observed no significant difference in the uptake of YoPro dye (Fig. S3C) or in the V_m of EpH4 cells cultured on soft or stiff substrata when we blocked connexin-43 hemichannels using the specific peptide TAT-gap19 (Abudara et al., 2014) (Fig. S3D,E). These data suggest that neither the mechanosensitive ion channel Piezo1 nor pannexin or connexin hemichannels are responsible

Journal of Cell Science (2021) 134, jcs256313. doi:10.1242/jcs.256313

for the regulation of V_m by substratum stiffness in mammary epithelial cells.

Intracellular Ca^{2+} is regulated by substratum stiffness (Kim et al., 2009). Furthermore, mammary tumors show alterations in the expression and activation of CaCCs (Hartzell et al., 2005; Ohkubo and Yamazaki, 2012). Breast tumors frequently show decreased expression of CFTR (Zhang et al., 2013), which is often mutated in cancer (Zhang et al., 2018) and can be gated by Ca^{2+} (Brennan et al., 2016). CaCCs can exert a depolarizing effect on the cell. Therefore, increased Ca^{2+} uptake in cells cultured on soft substrata might be expected to trigger the activation of such channels. To test this possibility, we first visualized intracellular Ca^{2+} in cells cultured on soft or stiff substrata using the fluorescent indicator, Calcium Green 1 (CG1). We observed higher CG1 intensity in EpH4 cells cultured on soft substrata compared to those on stiff substrata (Fig. 5A), in agreement with previous observations (Chiu et al., 2007). To determine whether Ca^{2+} is required for stiffness-dependent changes in V_m, we depleted intracellular Ca^{2+} using the membrane-permeable chelator BAPTA-AM (Fig. 5B). This treatment abolished the difference in V_m between cells cultured on soft and stiff substrata (Fig. 5C). These data suggest that Ca^{2+}-gated ion channels may be involved in the regulation of V_m by substratum stiffness. Not only does Ca^{2+} regulate V_m, but V_m can alter levels of intracellular Ca^{2+} via voltage-gated Ca^{2+} channels (VGCCs) (Catterall, 2011). Therefore, this feedback may serve as a way to amplify Ca^{2+} signaling in the context of mechanosensing in mammary epithelial cells. Accordingly, treatment with gramicidin significantly reduced the difference in CG1 intensity between EpH4 cells cultured on soft and stiff substrata (Fig. 5D,E). EpRas cells also showed a significant decrease in intracellular Ca^{2+} on stiff substrata (Fig. 5F). Taken together, these data suggest a connection between V_m, intracellular Ca^{2+} and substratum stiffness.

To determine the role of Ca^{2+}-gated ion channels, we blocked Ca^{2+}-gated potassium channels with iberiotoxin (IbTx) (Candia et al., 1992) or CaCCs with 5-nitro-2-(3-phenylpropylamino)benzoic acid (NPPB) (Ishikawa and Cook, 1993). We observed that IbTx did not affect V_m in EpH4 cells cultured on soft or stiff substrata (Fig. 5G). However, NPPB abolished the regulation of V_m by substratum stiffness in EpH4 cells (Fig. 5H), suggesting a role for CaCCs. Consistently, treatment with NPPB diminished the regulation of

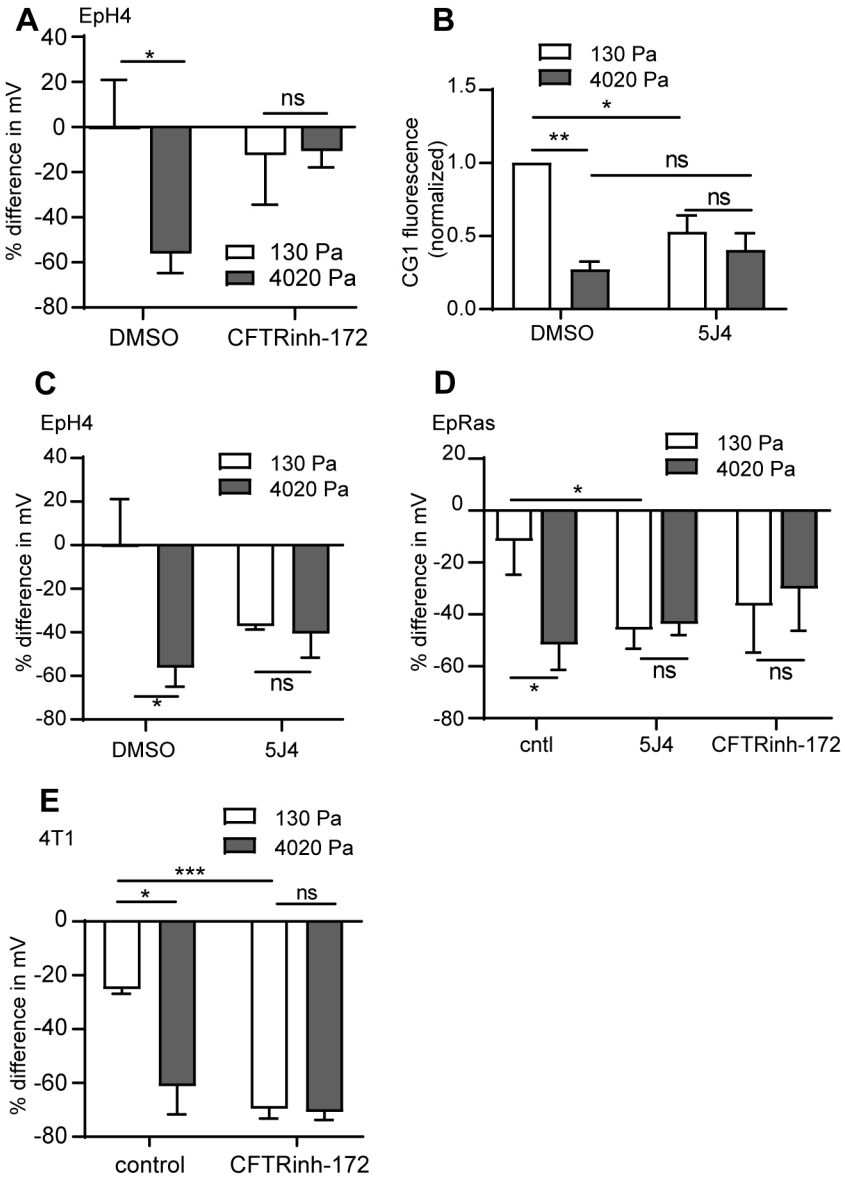

Fig. 6. CFTR is required for the regulation of V_m by substratum stiffness. (A) V_m of EpH4 cells cultured on soft or stiff substrata in the presence or absence of $CFTR_{inh}$-172. (B,C) CG1 fluorescence (B) or V_m (C) of EpH4 cells cultured on soft or stiff substrata in the presence or absence of 5J-4. (D,E) EpRas cells (D) or 4T1 cells (E) cultured on soft or stiff substrata in the presence or absence of $CFTR_{inh}$-172. Shown are mean+s.d. *P<0.05; **P<0.01; ***P<0.001; ns, not significant; as determined by an unpaired parametric t-test with Welch's correction. N=3 independent replicates.

Journal of Cell Science (2021) 134, jcs256313. doi:10.1242/jcs.256313

V_m by substratum stiffness in EpRas cells (Fig. 5I) and 4T1 cells (Fig. 5J,K). These data indicate that a CaCC is required for the regulation of V_m by substratum stiffness in mammary epithelial cells.

To identify which Ca^{2+}-gated ion channels are involved in the stiffness-induced changes in V_m, we treated cells with specific inhibitors. We found that the CFTR inhibitor $CFTR_{inh}$-172 (Verkman et al., 2013) blocked the ability of substratum stiffness to regulate V_m in EpH4 cells (Fig. 6A). It was previously reported that culture on soft substrata can induce the translocation of Stim1 from the endoplasmic reticulum to the plasma membrane in a manner dependent on inositol 1,4,5-trisphosphate (IP_3) (Chiu et al., 2008, 2007). At the plasma membrane, Stim1 interacts with Orai1, forming a CRAC. The resulting influx of Ca^{2+} might then activate Ca^{2+}-gated ion channels such as CFTR. Consistently, inhibiting CRAC current using the pharmacological inhibitor 5J4 (Kim et al., 2014) disrupted the regulation of intracellular Ca^{2+} (Fig. 6B) and V_m (Fig. 6C) by substratum stiffness. Further, inhibiting CFTR blocked the regulation of V_m by substratum stiffness in EpRas (Fig. 6D) and 4T1 (Fig. 6E) cells. Together, these data suggest that substratum stiffness regulates Orai1/Stim1 channels, which modulate Ca^{2+} levels that differentially gate CFTR, leading to changes in V_m (Fig. 7).

Constitutive activation of Ras is known to alter the expression of Ca^{2+}-gated ion channels (Huang and Rane, 1994). We therefore postulated that CaCCs might be differentially expressed between EpH4 and EpRas cells cultured on soft or stiff substrata. Consistently, we observed increased CFTR expression in EpRas cells cultured on stiff substrata, but not in EpH4 or 4T1 cells (Fig. S4). Although EpRas cells express more CFTR when cultured on stiff substrata than on soft substrata, V_m is still hyperpolarized compared with cells cultured on soft substrata. These data suggest that the regulation of V_m by substratum stiffness depends on CFTR activity, and not necessarily on expression levels.

DISCUSSION

The mechanical microenvironment plays an essential role in the regulation of cellular behaviors associated with normal development as well as cancer (Levental et al., 2009; Park et al., 2011; Tilghman et al., 2010; Ulrich et al., 2009; Zhang et al., 2011). For example, extracellular matrix stiffness regulates EMT (Tilghman et al., 2010), differentiation (Engler et al., 2006; Lee and Nelson, 2013; Pathak et al., 2014), proliferation (Tilghman et al., 2010; Ulrich et al., 2009) and apoptosis (Zhang et al., 2011). Consequently, tissue density is now recognized as a risk factor for tumor initiation and progression (Martin and Boyd, 2008). V_m regulates many of the same cellular behaviors as substratum stiffness (Adams and Levin, 2006, 2013; Beane et al., 2013; Chernet and Levin, 2014; Chowdhury et al., 2010; Engler et al., 2006; Ko et al., 2016; Kostic et al., 2009; Martinac, 2004; Pai et al., 2012, 2015; Sundelacruz et al., 2009; Tilghman et al., 2010; Ulrich et al., 2009; Wang, 2004; Zhang et al., 2011). Our data reveal, for the first time, that substratum stiffness controls V_m in mammary epithelial cells. These findings are not entirely unexpected. Cellular depolarization has been found to reduce the stiffness of vascular endothelial cells (Callies et al., 2011), and cells cultured on

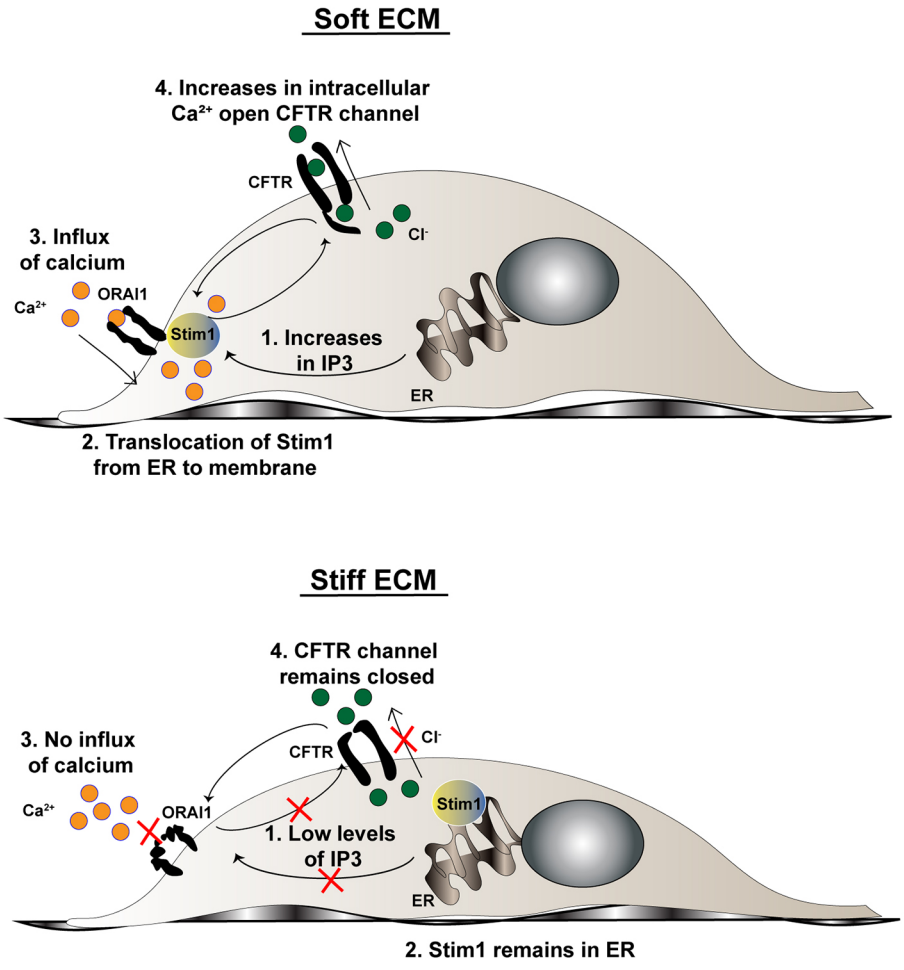

Fig. 7. Proposed mechanism by which the mechanical microenvironment regulates V_m. On soft substrata, upregulation of IP_3 triggers the translocation of Stim1 from the endoplasmic reticulum (ER) to the plasma membrane, where it associates with Orai1. Together, these proteins form a Ca^{2+} release-activated channel that conducts influx of Ca^{2+} (Chiu et al., 2008). Intracellular Ca^{2+} levels influence the gating of CFTR, resulting in differences in V_m between cells cultured on soft and stiff substrata.

Journal of Cell Science (2021) 134, jcs256313. doi:10.1242/jcs.256313

softer substrata are expected to have decreased stiffness (Tee et al., 2011). Therefore, although we focused our study on individual, functionally normal and tumorigenic mammary epithelial cells, we predict that substratum stiffness regulates V_m in other cell types as well. Future studies will investigate the effects of the mechanical properties of the microenvironment on V_m in 3D multicellular tissues.

We observed that depolarization correlates with a decrease in projected cell area, which is concordant with a decrease in the number of focal adhesions that are formed in cells on soft microenvironments (Katsumi et al., 2004; Levental et al., 2009; Pelham and Wang, 1997). Accordingly, we found that the ability of substratum stiffness to regulate V_m is lost upon inhibition of the key focal adhesion signaling protein, FAK. These findings suggest that substratum stiffness signals, at least in part, through focal adhesions to regulate V_m. Cytoskeletal tension caused by increased focal adhesion engagement gates mechanosensitive ion channels such as Piezo1 (Coste et al., 2010; Gudipaty et al., 2017; Pathak et al., 2014). However, we found that inhibiting Piezo channels had no effect on the ability of substratum stiffness to regulate V_m.

Instead, we observed that both Orai1/Stim1 and CFTR channels are required for substratum stiffness to modulate V_m. Specifically, we hypothesized that increased Ca^{2+} entry through Orai1/Stim1 channels in cells cultured on soft substrata opens CFTR, leading to outflux of negatively charged Cl^- ions, depolarizing the cell. Therefore, blocking either Orai1/Stim1 or CFTR channels would be expected to cause hyperpolarization of cells cultured on soft substrata. Indeed, we observed that blocking Orai1/Stim1 channels caused significant hyperpolarization of EpH4 and EpRas cells cultured on soft substrata, as anticipated. In addition, we observed that inhibiting CFTR hyperpolarized 4T1 cells cultured on soft substrata. However, inhibiting CFTR in EpH4 and EpRas cells unexpectedly caused depolarization of cells cultured on stiff substrata, with no effect in cells cultured on soft substrata. These differences in response to inhibiting CFTR correlate with a difference in change in cell spreading (Fig. S4), which emphasizes the tight coupling between cell morphology and V_m. From these data, we conclude that both Orai1/Stim1 and CFTR channels are required for the regulation of V_m by substratum stiffness. However, the exact activity of CFTR (direction of ion flow) appears to be cell type-specific, and could depend on many factors including Cl^- concentration in the extracellular media and cytoplasm.

Mammary epithelial cells express high levels of CFTR in apical membranes (Blaug et al., 2001). This channel has been proposed to play a role in regulating fluid flow (Blaug et al., 2001) as well as milk secretion and acid/base balance in the mammary gland (Ma et al., 2020). Furthermore, low CFTR expression at both the transcript and protein levels has been correlated with decreased survival and poor prognosis in breast cancer patients, and hypermethylation of the *CFTR* gene has been associated with cancer (Liu et al., 2020; Zhang et al., 2013). Based on these observations, CFTR has been proposed to function as a novel tumor suppressor (Ma et al., 2017b). However, studies that examined tumor formation in mouse xenograft models found that CFTR could exert either a tumor-suppressing or tumor-promoting role, depending upon whether the host tissues or cancer cells downregulated channel expression. This dichotomy emphasizes the importance of studying ion channel function within the context of the cellular microenvironment. Consistently, we observed upregulation of CFTR at the transcript level in EpRas cells cultured on stiff substrata, a hallmark of the tumor microenvironment. Future studies should focus on the signaling downstream of matrix mechanics that regulates the activity of CFTR and other ion channels.

MATERIALS AND METHODS

Cell culture

Mouse mammary epithelial cells (EpH4, SCp2 and SCg6) were maintained in 1:1 Dulbecco's modified Eagle medium (DMEM):F12 (Gibco) supplemented with 2% heat-inactivated fetal bovine serum (FBS; Atlanta Biologicals), 0.1% gentamicin (Gibco) and 5 µg/ml insulin (Sigma-Aldrich). The 4T1 mouse mammary carcinoma line was cultured in RPMI medium (GE Life Sciences) supplemented with 10% FBS and 0.1% gentamicin. EpRas cells are a Ras-transformed variant of EpH4 cells (Oft et al., 1996) and were cultured under the same conditions as the parental cell line. Human mammary epithelial cells (MCF10A) (Soule et al., 1990) were maintained in 1:1 DMEM:F12 supplemented with 5% horse serum (Atlanta Biologicals), 5 µg/ml insulin, 20 ng/ml epidermal growth factor (EGF; Sigma-Aldrich), 0.5 mg/ml hydrocortisone (Sigma-Aldrich), 100 ng/ml cholera toxin (Sigma-Aldrich) and 1× penicillin–streptomycin (Gibco). Cells were determined to be free of mycoplasma using a commercially available kit (Lonza).

Ca^{2+}-activated K^+ channels were inhibited using IbTx (500 nM, Tocris). Ca^{2+}-sensitive Cl^- currents were inhibited using NPPB (50 µM, Tocris). CFTR channels were inhibited using $CFTR_{inh}$-172 (17.5 µM, Tocris). Stim1/Orai1 channels were inhibited using 5J4 (20 µM, Tocris). Piezo1 channels were inhibited using $GdCl_3$ (200 µM, Alfa Aesar). Cx43 (also known as GJA1) hemichannels were inhibited using the peptide TAT-gap19 (Abudara et al., 2014) (50 µM, Tocris). FAK was inhibited using PF-573228 (5 µM, Sigma-Aldrich). All inhibitors were applied to cells for 24 h. Intracellular Ca^{2+} was chelated using BAPTA-AM (3 µM, Thermo Fisher Scientific), which was applied to cells for 24 h.

Preparation of polyacrylamide substrata

Polyacrylamide substrata were prepared as described previously (Lee and Nelson, 2013). Briefly, glass coverslips were cross-linked with a solution of 12.5% (w/v) acrylamide monomer (Bio-Rad), 0.5% ammonium persulfate (Sigma-Aldrich), 0.1% N,N,N′,N′-tetramethylethylenediamine (TEMED; Sigma-Aldrich) and bis-acrylamide (Bio-Rad). The elastic moduli of the gels were tuned by altering the concentration of bis-acrylamide cross-linker. Substrata of 130, 910, 2030 or 4020 Pa were prepared using bis-acrylamide concentrations (w/v) of 0.5%, 1.5%, 3.0% or 17.5%, respectively (Lee and Nelson, 2013). To promote cellular adhesion, the gels were functionalized with 0.2 mg/ml fibronectin (Corning Life Sciences) using sulfosuccinimidyl-6-(4′-azido-2′-nitrophenyl-amino)-hexanoate (sulfo-SANPAH; Thermo Fisher Scientific). Mammary epithelial cells were seeded onto the substrata at a density of ∼280 cells/mm^2 and cultured for 16–24 h before imaging. Care was taken to image the cells after adhesion to the substrata but before mitosis to enable analysis of single cells.

Microcontact-printed substrata

We used a microfabrication-based approach (Tan et al., 2004) to control the projected area of cells by confining adhesion to a defined island of fibronectin. Briefly, stamps of polydimethylsiloxane (PDMS; Sylgard 184) were sterilized using 200-proof ethanol, then coated with 25 µg/ml fibronectin in PBS overnight. Sterilized water was used to remove excess fibronectin from the stamps, which were then dried under compressed nitrogen. The stamps were then applied onto custom-made, UV/ozone-treated, PDMS-coated glass-bottom tissue culture dishes for at least 15 min to allow transfer of fibronectin from the stamp to the culture dish. Unstamped regions were blocked with 1% Synperonic F108 (Fluka) in PBS. Cells were seeded onto the fibronectin islands at a concentration of ∼3×10^5 cells/ml for 2–3 h. Nonadherent cells were removed by washing once with culture medium. Adherent cells were cultured for ∼16 h on the islands. We compared unconstrained cells to those confined to circular (16 µm-diameter) fibronectin islands. These projected areas were comparable to those of cells on stiff (519±54 µm^2) or soft (199±40 µm^2) substrata, respectively.

Immunoblotting analysis

EpH4 cells were cultured for 24 h in the presence of different concentrations of PF-573228. Cells were then treated with RIPA lysis buffer (Thermo Fisher Scientific) supplemented with protease inhibitor (Roche). The Pierce

Bicinchoninic Acid (BCA) Protein Assay Kit (Thermo Fisher Scientific) was used to measure protein concentration. Samples were heated at 95°C for 10 min with LDS sample buffer and reducing agent (Thermo Fisher Scientific), resolved by electrophoresis on a 4–12% bis-tris gel and transferred onto nitrocellulose membranes. The membranes were blocked in 5% nonfat milk in TBST [0.1% Tween 20 (Sigma-Aldrich) in Tris-buffered saline] and incubated overnight at 4°C in TBST containing antibodies specific to FAK (1:1000; 3285S, Cell Signaling Technology), pY397-FAK (1:1000; 44-625G, Cell Signaling Technology) or horseradish peroxidase-conjugated GAPDH (1:5000; Cell Signaling Technology).

Quantitative RT-PCR analysis

Standard Trizol extraction (Invitrogen) procedures were used to isolate total RNA from cells cultured on soft or stiff substrata. A commercially available kit (Verso cDNA synthesis kit, Thermo Fisher Scientific) was used to reverse-transcribe the RNA into cDNA. A StepOnePlus Realtime PCR System (Applied Biosystems) was used to perform quantitative RT-PCR using iTaq Universal SYBR Green SuperMix (Bio-Rad). CFTR expression was evaluated using primers validated by BLAST (F, 5′-CAGCGATGGA-GAAAATGATTG-3′; R, 5′-GGGAAGCACAGATAGAAAGAC-3′) and analysis of standard curve. Target gene expression was normalized to that of 18S rRNA in each sample using previously published primer sequences (Han et al., 2018).

V_m measurements, Ca^{2+} visualization and YoPro uptake assay

The reporter dye $DiBac_4(3)$ (2 µg/ml in culture medium) was used to estimate cellular V_m. This dye more easily crosses the plasma membrane of depolarized (more positively charged) cells in a manner in which the percentage increase in fluorescence intensity is approximately linearly proportional to the millivolt increase in V_m depolarization (Bräuner et al., 1984; Klapperstück et al., 2013; Silver et al., 2020; Yamada et al., 2001). $DiBac_4(3)$ is used in a live-cell assay that requires an equilibrium to be reached across the cell membrane and, as a result, remains in the culture medium during imaging. All samples were imaged in culture medium containing 2% FBS to reduce background autofluorescence caused by higher serum concentrations. Gramicidin-treated cells were prepared by adding gramicidin (3 µg/ml, Sigma-Aldrich) and $DiBac_4(3)$ (2 µg/ml) to the culture medium. EpH4, EpRas, SCp2, SCg6 and MCF10A cells were incubated in these solutions for 5 h before imaging; 4T1 cells, which were found to be more sensitive to gramicidin, were incubated for 2 h prior to imaging. Intracellular Ca^{2+} was visualized using CG1 (10 µM, Thermo Fisher Scientific) applied for 24 h, then washed 3× with culture medium prior to imaging. To visualize Ca^{2+} in cells in which V_m had been disrupted, gramicidin was applied at 0.5 µM or 1 µM over a 24-h period. To assess YoPro uptake, cells were washed 3× in PBS, then incubated in YO-PRO™-1 (Thermo Fisher Scientific) diluted 1:1000 in PBS for 15 min at room temperature in the dark prior to imaging. To measure cell height and volume, EpH4 cells were cultured on soft or stiff substrata for 24 h, treated with Calcein-AM dye for 30 min, and then washed 3× with culture medium. Prior to imaging, samples were washed at least 3× to remove excess dye (CG1, YoPro and Calcein-AM dye).

Microscopy

All samples were imaged using a Nikon Eclipse Ti-U inverted fluorescence microscope (Melville, NY) equipped with an ORCA charge-coupled device camera (Hamamatsu, Japan). Images were taken at 488 nm using a 20× air objective. An image of cell-free substratum (glass or hydrogel) was used to subtract background fluorescence prior to image analysis. Mean fluorescence intensity was determined by taking the mean fluorescence of cells imaged on either soft or stiff substrata for both the gramicidin-treated and untreated samples. Percentage difference between the gramicidin-treated and untreated samples on each substratum was then calculated, normalizing to the gramicidin-treated samples. This percentage difference corresponded to V_m in mV. Measurements were performed on at least 20 cells across three separate biological replicates for both gramicidin-treated and untreated samples. For cell height measurements, confocal stacks were taken of at least 30 cells using a Nikon A1 laser-scanning confocal microscope.

Acknowledgements

We would like to thank members of the Tissue Morphodynamics Laboratory for their input and expertise.

Competing interests

The authors declare no competing or financial interests.

Author contributions

Conceptualization: B.B.S., C.M.N.; Methodology: B.B.S.; Formal analysis: E.M.R.; Investigation: B.B.S., S.X.Z.; Writing - original draft: B.B.S.; Writing - review & editing: C.M.N.; Supervision: C.M.N.; Project administration: C.M.N.; Funding acquisition: C.M.N.

Funding

This work was supported, in part, by grants from the National Institutes of Health (NIH) [CA187692, CA214292] and a Faculty Scholars Award from the Howard Hughes Medical Institute. B.B.S. was supported in part by the National Science Foundation Graduate Research Fellowship Program. E.M.R. was supported in part by an NIH National Research Service Award F30 (GM134602). Deposited in PMC for release after 12 months.

References

Abudara, V., Bechberger, J., Freitas-Andrade, M., De Bock, M., Wang, N., Bultynck, G., Naus, C. C., Leybaert, L. and Giaume, C. (2014). The connexin43 mimetic peptide Gap19 inhibits hemichannels without altering gap junctional communication in astrocytes. *Front. Cell Neurosci.* **8**, 306. doi:10.3389/fncel.2014.00306

Adams, D. S. and Levin, M. (2006). Inverse drug screens: a rapid and inexpensive method for implicating molecular targets. *Genesis* **44**, 530-540. doi:10.1002/dvg.20246

Adams, D. S. and Levin, M. (2013). Endogenous voltage gradients as mediators of cell-cell communication: strategies for investigating bioelectrical signals during pattern formation. *Cell Tissue Res.* **352**, 95-122. doi:10.1007/s00441-012-1329-4

Adams, D. S., Masi, A. and Levin, M. (2007). H+ pump-dependent changes in membrane voltage are an early mechanism necessary and sufficient to induce Xenopus tail regeneration. *Development* **134**, 1323-1335. doi:10.1242/dev.02812

Batra, N., Burra, S., Siller-Jackson, A. J., Gu, S., Xia, X., Weber, G. F., DeSimone, D., Bonewald, L. F., Lafer, E. M., Sprague, E. et al. (2012). Mechanical stress-activated integrin α5β1 induces opening of connexin 43 hemichannels. *Proc. Natl. Acad. Sci. USA* **109**, 3359-3364. doi:10.1073/pnas.1115967109

Beane, W. S., Morokuma, J., Adams, D. S. and Levin, M. (2011). A chemical genetics approach reveals H, K-ATPase-mediated membrane voltage is required for planarian head regeneration. *Chem. Biol.* **18**, 77-89. doi:10.1016/j.chembiol.2010.11.012

Beane, W. S., Morokuma, J., Lemire, J. M. and Levin, M. (2013). Bioelectric signaling regulates head and organ size during planarian regeneration. *Development* **140**, 313-322. doi:10.1242/dev.086900

Blaug, S., Hybiske, K., Cohn, J., Firestone, G. L., Machen, T. E. and Miller, S. S. (2001). ENaC- and CFTR-dependent ion and fluid transport in mammary epithelia. *Am. J. Physiol. Cell Phys.* **281**, C633-C648. doi:10.1152/ajpcell.2001.281.2.C633

Bräuner, T., Hülser, D. F. and Strasser, R. J. (1984). Comparative measurements of membrane potentials with microelectrodes and voltage-sensitive dyes. *Biochim. Biophys. Acta* **771**, 208-216. doi:10.1016/0005-2736(84)90535-2

Brennan, S. C., Wilkinson, W. J., Tseng, H.-E., Finney, B., Monk, B., Dibble, H., Quilliam, S., Warburton, D., Galietta, L. J., Kemp, P. J. et al. (2016). The extracellular calcium-sensing receptor regulates human fetal lung development via CFTR. *Sci. Rep.* **6**, 21975. doi:10.1038/srep21975

Califano, J. P. and Reinhart-King, C. A. (2010). Substrate stiffness and cell area predict cellular traction stresses in single cells and cells in contact. *Cell. Mol. Bioeng.* **3**, 68-75. doi:10.1007/s12195-010-0102-6

Callies, C., Fels, J., Liashkovich, I., Kliche, K., Jeggle, P., Kusche-Vihrog, K. and Oberleithner, H. (2011). Membrane potential depolarization decreases the stiffness of vascular endothelial cells. *J. Cell Sci.* **124**, 1936-1942. doi:10.1242/jcs.084657

Candia, S., Garcia, M. L. and Latorre, R. (1992). Mode of action of iberiotoxin, a potent blocker of the large conductance Ca(2+)-activated K+ channel. *Biophys. J.* **63**, 583-590. doi:10.1016/S0006-3495(92)81630-2

Catterall, W. A. (2011). Voltage-gated calcium channels. *Cold Spring Harbor Pers. Biol.* **3**, a003947. doi:10.1101/cshperspect.a003947

Chernet, B. T. and Levin, M. (2013). Transmembrane voltage potential is an essential cellular parameter for the detection and control of tumor development in a Xenopus model. *Dis. Model. Mech.* **6**, 595-607. doi:10.1242/dmm.010835

Chernet, B. T. and Levin, M. (2014). Transmembrane voltage potential of somatic cells controls oncogene-mediated tumorigenesis at long-range. *Oncotarget* **5**, 3287. doi:10.18632/oncotarget.1935

Chiu, W.-T., Wang, Y.-H., Tang, M.-J. and Shen, M.-R. (2007). Soft substrate induces apoptosis by the disturbance of Ca2+ homeostasis in renal epithelial LLC–PK1 cells. *J. Cell Physiol.* **212**, 401-410. doi:10.1002/jcp.21037

Chiu, W.-T., Tang, M.-J., Jao, H.-C. and Shen, M.-R. (2008). Soft substrate up-regulates the interaction of STIM1 with store-operated Ca2+ channels that lead to normal epithelial cell apoptosis. *Mol. Biol. Cell* **19**, 2220-2230. doi:10.1091/mbc.e07-11-1170

Chowdhury, F., Na, S., Li, D., Poh, Y.-C., Tanaka, T. S., Wang, F. and Wang, N. (2010). Material properties of the cell dictate stress-induced spreading and differentiation in embryonic stem cells. *Nat. Mat.* **9**, 82-88. doi:10.1038/nmat2563

Coste, B., Mathur, J., Schmidt, M., Earley, T. J., Ranade, S., Petrus, M. J., Dubin, A. E. and Patapoutian, A. (2010). Piezo1 and Piezo2 are essential components of distinct mechanically activated cation channels. *Science* **330**, 55-60. doi:10.1126/science.1193270

Desprez, P., Roskelley, C., Campisi, J. and Bissell, M. (1993). Isolation of functional cell lines from a mouse mammary epithelial cell strain: the importance of basement membrane and cell-cell interaction. *Mol. Cell. Differ.* **1**, 99-110.

Engler, A. J., Sen, S., Sweeney, H. L. and Discher, D. E. (2006). Matrix elasticity directs stem cell lineage specification. *Cell* **126**, 677-689. doi:10.1016/j.cell.2006.06.044

Ermakov, Y. A., Kamaraju, K., Sengupta, K. and Sukharev, S. (2010). Gadolinium ions block mechanosensitive channels by altering the packing and lateral pressure of anionic lipids. *Biophys. J.* **98**, 1018-1027. doi:10.1016/j.bpj.2009.11.044

Fu, J., Wang, Y.-K., Yang, M. T., Desai, R. A., Yu, X., Liu, Z. and Chen, C. S. (2010). Mechanical regulation of cell function with geometrically modulated elastomeric substrates. *Nat. Methods* **7**, 733. doi:10.1038/nmeth.1487

Guan, J.-L. (2010). Integrin signaling through FAK in the regulation of mammary stem cells and breast cancer. *IUBMB Life* **62**, 268-276. doi:10.1002/iub.303

Gudipaty, S. A., Lindblom, J., Loftus, P. D., Redd, M. J., Edes, K., Davey, C., Krishnegowda, V. and Rosenblatt, J. (2017). Mechanical stretch triggers rapid epithelial cell division through Piezo1. *Nature* **543**, 118-121. doi:10.1038/nature21407

Han, S., Pang, M.-F. and Nelson, C. M. (2018). Substratum stiffness tunes proliferation downstream of Wnt3a in part by regulating integrin-linked kinase and frizzled-1. *J. Cell Sci.* **131**, jcs210476. doi:10.1242/jcs.210476

Hartzell, C., Putzier, I. and Arreola, J. (2005). Calcium-activated chloride channels. *Annu. Rev. Physiol.* **67**, 719-758. doi:10.1146/annurev.physiol.67.032003.154341

Huang, Y. and Rane, S. G. (1994). Potassium channel induction by the Ras/Raf signal transduction cascade. *J. Biol. Chem.* **269**, 31183-31189. doi:10.1016/S0021-9258(18)47407-8

Ishikawa, T. and Cook, D. I. (1993). A Ca 2+-activated Cl– current in sheep parotid secretory cells. *J. Memb. Biol.* **135**, 261-271. doi:10.1007/BF00211098

Katsumi, A., Orr, A. W., Tzima, E. and Schwartz, M. A. (2004). Integrins in mechanotransduction. *J. Biol. Chem.* **279**, 12001-12004. doi:10.1074/jbc.R300038200

Kelkar, D. A. and Chattopadhyay, A. (2007). The gramicidin ion channel: a model membrane protein. *Biochim. Biophys. Acta Biomembr.* **1768**, 2011-2025. doi:10.1016/j.bbamem.2007.05.011

Kim, T.-J., Seong, J., Ouyang, M., Sun, J., Lu, S., Hong, J. P., Wang, N. and Wang, Y. (2009). Substrate rigidity regulates Ca2+ oscillation via RhoA pathway in stem cells. *J. Cell. Physiol.* **218**, 285-293. doi:10.1002/jcp.21598

Kim, K.-D., Srikanth, S., Tan, Y.-V., Yee, M.-K., Jew, M., Damoiseaux, R., Jung, M. E., Shimizu, S., An, D. S., Ribalet, B. et al. (2014). Calcium signaling via Orai1 is essential for induction of the nuclear orphan receptor pathway to drive Th17 differentiation. *J. Immunol.* **192**, 110-122. doi:10.4049/jimmunol.1302586

Klapperstück, T., Glanz, D., Hanitsch, S., Klapperstück, M., Markwardt, F. and Wohlrab, J. (2013). Calibration procedures for the quantitative determination of membrane potential in human cells using anionic dyes. *Cytometry Part A* **83**, 612-626. doi:10.1002/cyto.a.22300

Ko, P., Kim, D., You, E., Jung, J., Oh, S., Kim, J., Lee, K.-H. and Rhee, S. (2016). Extracellular matrix rigidity-dependent sphingosine-1-phosphate secretion regulates metastatic cancer cell invasion and adhesion. *Sci. Rep.* **6**, 1-13.

Kobayashi, T. and Sokabe, M. (2010). Sensing substrate rigidity by mechanosensitive ion channels with stress fibers and focal adhesions. *Curr. Opin. Cell Biol.* **22**, 669-676. doi:10.1016/j.ceb.2010.08.023

Kong, H. J., Polte, T. R., Alsberg, E. and Mooney, D. J. (2005). FRET measurements of cell-traction forces and nano-scale clustering of adhesion ligands varied by substrate stiffness. *Proc. Natl. Acad. Sci. USA* **102**, 4300-4305. doi:10.1073/pnas.0405873102

Kostic, A., Lynch, C. D. and Sheetz, M. P. (2009). Differential matrix rigidity response in breast cancer cell lines correlates with the tissue tropism. *PLoS ONE* **4**, e6361. doi:10.1371/journal.pone.0006361

Lee, K. and Nelson, C. M. (2014). Determining the role of matrix compliance in the differentiation of mammary stem cells. In *Biomimetics and Stem Cells: Methods and Protocols* (Methods in Molecular Biology series), (eds G. Vunjak-Novakovic and K. Turksen), vol. 1202, pp. 79-94. New York: Springer.

Lee, K. A., Chen, Q. K., Lui, C., Cichon, M. A., Radisky, D. C. and Nelson, C. M. (2012). Matrix compliance regulates Rac1b localization, NADPH oxidase assembly, and epithelial–mesenchymal transition. *Mol. Biol. Cell* **23**, 4097-4108. doi:10.1091/mbc.e12-02-0166

Levental, K. R., Yu, H., Kass, L., Lakins, J. N., Egeblad, M., Erler, J. T., Fong, S. F. T., Csiszar, K., Giaccia, A., Weninger, W. et al. (2009). Matrix crosslinking forces tumor progression by enhancing integrin signaling. *Cell* **139**, 891-906. doi:10.1016/j.cell.2009.10.027

Levin, M. (2014). Molecular bioelectricity: how endogenous voltage potentials control cell behavior and instruct pattern regulation in vivo. *Mol. Biol. Cell* **25**, 3835-3850. doi:10.1091/mbc.e13-12-0708

Liu, K., Dong, F., Gao, H., Guo, Y., Li, H., Yang, F., Zhao, P., Dai, Y., Wang, J., Zhou, W. et al. (2020). Promoter hypermethylation of the CFTR gene as a novel diagnostic and prognostic marker of breast cancer. *Cell Biol. Int.* **44**, 603-609. doi:10.1002/cbin.11260

Ma, K., Wang, H., Yu, J., Wei, M. and Xiao, Q. (2017a). New insights on the regulation of Ca2+–activated chloride channel TMEM16A. *J. Cell. Physiol.* **232**, 707-716. doi:10.1002/jcp.25621

Ma, M., Wang, C., Glicksberg, B. S., Schadt, E. E., LI, S. D. and Chen, R. (2017b). Identify cancer driver genes through shared mendelian disease pathogenic variants and cancer somatic mutations. *Pac. Symp. Biocomput.* **2017**, 473-484. doi:10.1142/9789813207813_0044

Ma, Z., Yuan, D., Cheng, X., Tuo, B., Liu, X. and Li, T. (2020). Function of ion transporters in maintaining acid-base homeostasis of the mammary gland and the pathophysiological role in breast cancer. *Am. J. Physiol. Regul. Integ. Comp. Physiol.* **318**, R98-R111. doi:10.1152/ajpregu.00202.2019

Martin, L. J. and Boyd, N. F. (2008). Potential mechanisms of breast cancer risk associated with mammographic density: hypotheses based on epidemiological evidence. *Breast Cancer Res.* **10**, 1-14. doi:10.1186/bcr1831

Martinac, B. (2004). Mechanosensitive ion channels: molecules of mechanotransduction. *J. Cell Sci.* **117**, 2449-2460. doi:10.1242/jcs.01232

Oft, M., Peli, J., Rudaz, C., Schwarz, H., Beug, H. and Reichmann, E. (1996). TGF-beta1 and Ha-Ras collaborate in modulating the phenotypic plasticity and invasiveness of epithelial tumor cells. *Genes Dev.* **10**, 2462-2477. doi:10.1101/gad.10.19.2462

Ohkubo, T. and Yamazaki, J. (2012). T-type voltage-activated calcium channel Cav3.1, but not Cav3.2, is involved in the inhibition of proliferation and apoptosis in MCF-7 human breast cancer cells. *Int. J. Oncol.* **41**, 267-275. doi:10.3892/ijo.2012.1422

Pai, V. P., Aw, S., Shomrat, T., Lemire, J. M. and Levin, M. (2012). Transmembrane voltage potential controls embryonic eye patterning in Xenopus laevis. *Development* **139**, 313-323. doi:10.1242/dev.073759

Pai, V. P., Lemire, J. M., Chen, Y., Lin, G. and Levin, M. (2015). Local and long-range endogenous resting potential gradients antagonistically regulate apoptosis and proliferation in the embryonic CNS. *Int. J. Dev. Biol* **59**, 327-340. doi:10.1387/ijdb.150197ml

Park, J. S., Chu, J. S., Tsou, A. D., Diop, R., Tang, Z., Wang, A. and Li, S. (2011). The effect of matrix stiffness on the differentiation of mesenchymal stem cells in response to TGF-β. *Biomaterials* **32**, 3921-3930. doi:10.1016/j.biomaterials.2011.02.019

Paszek, M. J., Zahir, N., Johnson, K. R., Lakins, J. N., Rozenberg, G. I., Gefen, A., Reinhart-King, C. A., Margulies, S. S., Dembo, M., Boettiger, D. et al. (2005). Tensional homeostasis and the malignant phenotype. *Cancer Cell* **8**, 241-254. doi:10.1016/j.ccr.2005.08.010

Patel, D., Zhang, X. and Veenstra, R. D. (2014). Connexin hemichannel and pannexin channel electrophysiology: how do they differ? *FEBS Lett.* **588**, 1372-1378. doi:10.1016/j.febslet.2013.12.023

Pathak, M. M., Nourse, J. L., Tran, T., Hwe, J., Arulmoli, J., Le, D. T. T., Bernardis, E., Flanagan, L. A. and Tombola, F. (2014). Stretch-activated ion channel Piezo1 directs lineage choice in human neural stem cells. *Proc. Natl. Acad. Sci. USA* **111**, 16148-16153. doi:10.1073/pnas.1409802111

Pelham, R. J. and Wang, Y.-L. (1997). Cell locomotion and focal adhesions are regulated by substrate flexibility. *Proc. Natl. Acad. Sci. USA* **94**, 13661-13665. doi:10.1073/pnas.94.25.13661

Provenzano, P. P., Inman, D. R., Eliceiri, K. W. and Keely, P. J. (2009). Matrix density-induced mechanoregulation of breast cell phenotype, signaling and gene expression through a FAK–ERK linkage. *Oncogene* **28**, 4326-4343. doi:10.1038/onc.2009.299

Rhee, S., Jiang, H., Ho, C.-H. and Grinnell, F. (2007). Microtubule function in fibroblast spreading is modulated according to the tension state of cell–matrix interactions. *Proc. Natl. Acad. Sci. USA* **104**, 5425-5430. doi:10.1073/pnas.0608030104

Sheppard, D. N. and Welsh, M. J. (1999). Structure and function of the CFTR chloride channel. *Phys. Rev.* **79**, S23-S45. doi:10.1152/physrev.1999.79.1.S23

Silver, B. B., Wolf, A. E., Lee, J., Pang, M.-F. and Nelson, C. M. (2020). Epithelial tissue geometry directs emergence of bioelectric field and pattern of proliferation. *Mol. Biol. Cell* **31**, 1691-1702. doi:10.1091/mbc.E19-12-0719

Slack-Davis, J. K., Martin, K. H., Tilghman, R. W., Iwanicki, M., Ung, E. J., Autry, C., Luzzio, M. J., Cooper, B., Kath, J. C., Roberts, W. G. et al. (2007). Cellular characterization of a novel focal adhesion kinase inhibitor. *J. Biol. Chem.* **282**, 14845-14852. doi:10.1074/jbc.M606695200

Soule, H. D., Maloney, T. M., Wolman, S. R., Peterson, W. D., Brenz, R., McGrath, C. M., Russo, J., Pauley, R. J., Jones, R. F. and Brooks, S. (1990). Isolation and characterization of a spontaneously immortalized human breast epithelial cell line, MCF-10. *Cancer Res.* **50**, 6075-6086.

Sundelacruz, S., Levin, M. and Kaplan, D. L. (2009). Role of membrane potential in the regulation of cell proliferation and differentiation. *Stem Cell Rev. Rep.* **5**, 231-246. doi:10.1007/s12015-009-9080-2

Tan, J. L., Liu, W., Nelson, C. M., Raghavan, S. and Chen, C. S. (2004). Simple approach to micropattern cells on common culture substrates by tuning substrate wettability. *Tissue Eng.* **10**, 865-872. doi:10.1089/1076327041348365

Tee, S.-Y., Fu, J., Chen, C. S. and Janmey, P. A. (2011). Cell shape and substrate rigidity both regulate cell stiffness. *Biophys. J.* **100**, L25-L27. doi:10.1016/j.bpj.2010.12.3744

Tilghman, R. W., Cowan, C. R., Mih, J. D., Koryakina, Y., Gioeli, D., Slack-Davis, J. K., Blackman, B. R., Tschumperlin, D. J. and Parsons, J. T. (2010). Matrix rigidity regulates cancer cell growth and cellular phenotype. *PLoS ONE* **5**, e12905. doi:10.1371/journal.pone.0012905

Ulrich, T. A., de Juan Pardo, E. M. and Kumar, S. (2009). The mechanical rigidity of the extracellular matrix regulates the structure, motility, and proliferation of glioma cells. *Cancer Res.* **69**, 4167-4174. doi:10.1158/0008-5472.CAN-08-4859

Verkman, A. S., Synder, D., Tradtrantip, L., Thiagarajah, J. R. and Anderson, M. O. (2013). CFTR inhibitors. *Curr. Pharm. Des.* **19**, 3529-3541. doi:10.2174/13816128113199990321

Wang, Z. (2004). Roles of K+ channels in regulating tumour cell proliferation and apoptosis. *Pflügers Archiv.* **448**, 274-286. doi:10.1007/s00424-004-1258-5

Wang, H.-B., Dembo, M. and Wang, Y.-L. (2000). Substrate flexibility regulates growth and apoptosis of normal but not transformed cells. *Am. J. Physiol. Cell Phys.* **279**, C1345-C1350. doi:10.1152/ajpcell.2000.279.5.C1345

Wu, J., Lewis, A. H. and Grandl, J. (2017). Touch, tension, and transduction–the function and regulation of Piezo ion channels. *Trends Biochem. Sci.* **42**, 57-71. doi:10.1016/j.tibs.2016.09.004

Yamada, A., Gaja, N., Ohya, S., Muraki, K., Narita, H., Ohwada, T. and Imaizumi, Y. (2001). Usefulness and limitation of DiBAC4(3), a voltage-sensitive fluorescent dye, for the measurement of membrane potentials regulated by recombinant large conductance Ca2+-activated K+ channels in HEK293 cells. *Jpn. J. Pharmacol.* **86**, 342-350. doi:10.1254/jjp.86.342

Yang, M. and Brackenbury, W. J. (2013). Membrane potential and cancer progression. *Front. Physiol.* **4**, 185. doi:10.3389/fphys.2013.00185

Zhang, Y.-H., Zhao, C.-Q., Jiang, L.-S. and Dai, L.-Y. (2011). Substrate stiffness regulates apoptosis and the mRNA expression of extracellular matrix regulatory genes in the rat annular cells. *Matrix Biol.* **30**, 135-144. doi:10.1016/j.matbio.2010.10.008

Zhang, J. T., Jiang, X. H., Xie, C., Cheng, H., Da Dong, J., Wang, Y., Fok, K. L., Zhang, X. H., Sun, T. T. and Tsang, L. L. (2013). Downregulation of CFTR promotes epithelial-to-mesenchymal transition and is associated with poor prognosis of breast cancer. *Biochim. Biophs. Acta Mol. Cell Res.* **1833**, 2961-2969.

Zhang, J., Wang, Y., Jiang, X. and Chan, H. C. (2018). Cystic fibrosis transmembrane conductance regulator-emerging regulator of cancer. *Cell Mol. Life Sci.* **75**, 1737-1756. doi:10.1007/s00018-018-2755-6

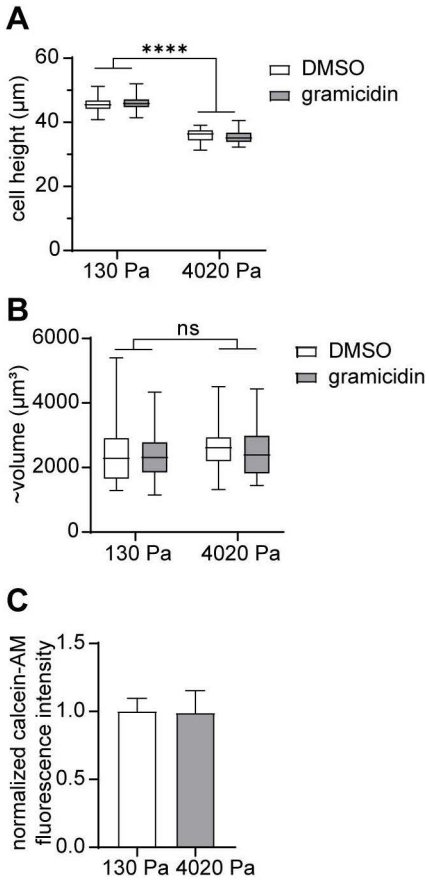

Figure S1. Substratum stiffness has minimal effects on cell height. (**A**) Height and (**B**) volume of EpH4 cells cultured on soft or stiff substratum in the presence or absence of gramicidin. Shown are minimum, maximum, and mean values. (**C**) Intensity of calcein-AM fluorescence of cells on soft or stiff substratum. ****, P<0.0001; as determined by an unpaired parametric t-test with Welch's correction.

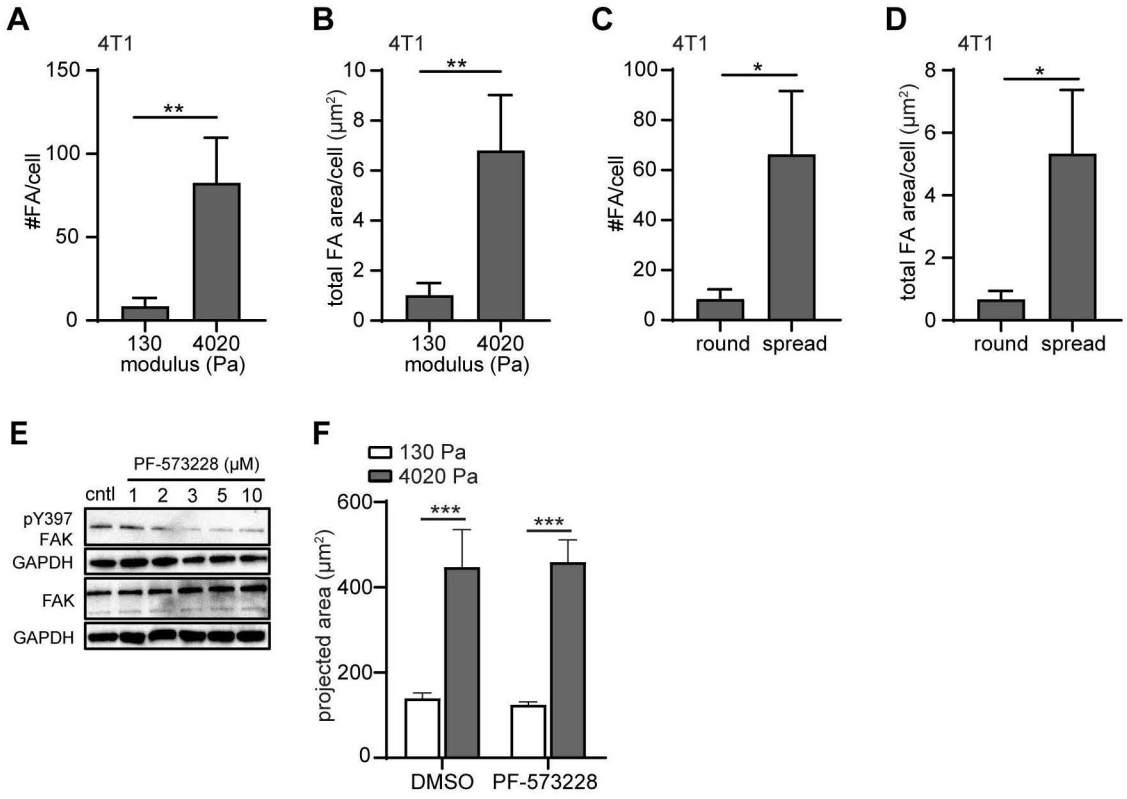

Figure S2. Substratum stiffness regulates focal adhesions. Average (**A**) number and (**B**) total area of focal adhesions in 4T1 cells cultured on soft (17 cells) or stiff (14 cells) substrata. Average (**C**) number and (**D**) total area of focal adhesions in round (16 cells) or spread (8 cells) 4T1 cells cultured on micropatterned substrata. (**E**) Immunoblot showing levels of pFAK, total FAK, and GAPDH in EpH4 cells treated with different concentrations of PF-573228.

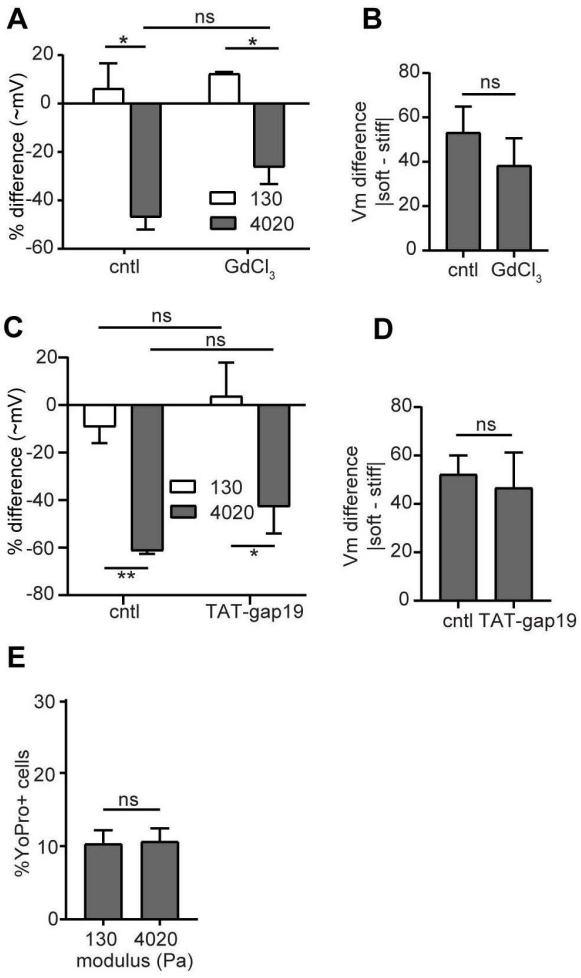

Figure S3. Piezo1 and connexin hemichannels are not required for the regulation of Vm by substratum stiffness. (**A**) Vm measurements of EpH4 cells cultured on soft or stiff substrata treated with or without $GdCl_3$. (**B**) Difference in Vm between cells cultured on soft or stiff substrata treated with or without $GdCl_3$. (**C**) Vm of EpH4 cells cultured on soft or stiff substrata treated with or without TAT-gap19. (**D**) Difference in Vm between cells cultured on soft or stiff substrata treated with or without TAT-gap19. (**E**) Percentage of EpH4 cells showing YoPro dye uptake on soft or stiff substrata. Scale bars represent 25 μm. Shown are mean + SD. *, $P<0.05$; **, $P<0.01$; as determined by an unpaired parametric t-test with Welch's correction. N=3 independent replicates.

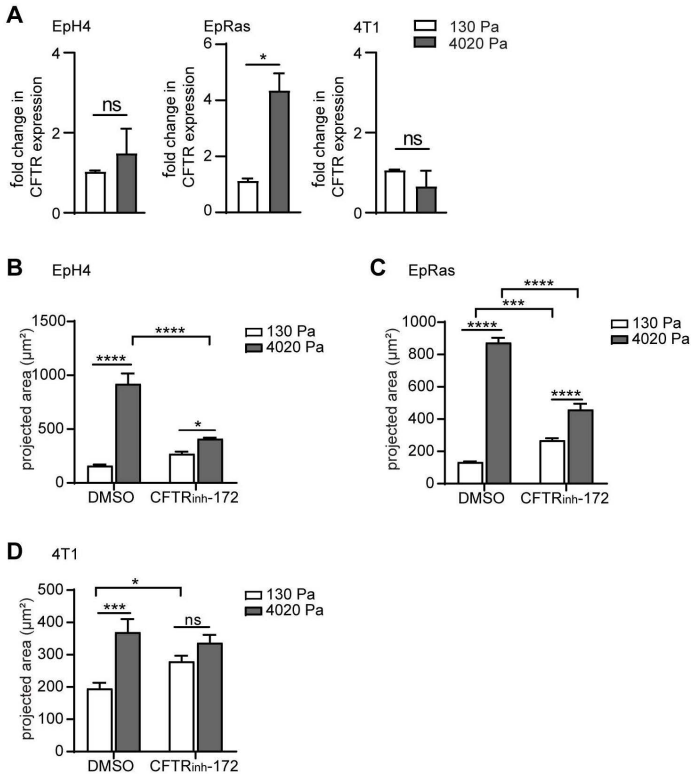

Figure S4. Ras-transformed cells upregulate CFTR on stiff substrata. (**A**) qRT-PCR analysis for CFTR in EpH4, EpRas, and 4T1 cells cultured on soft (130 Pa) or stiff (4020 Pa) substrata. Projected area of (**B**) EpH4, (**C**) EpRas, and (**D**) 4T1 cells cultured on soft or stiff substrata in the presence or absence of $CFTR_{inh}$-172. Shown are mean + SD. *, $P<0.05$; as determined by an unpaired parametric t-test with Welch's correction. N=3 independent replicates.